Anal. Bioanal. Electrochem., Vol. 16, No. 11, 2024, 978-999
https://www.doi.org/10.22034/abec.2024.718624

Analytical & Bioanalytical Electrochemistry

Full Paper

Corrosion Inhibition of Cocamidopropyl Betaine on Aluminum 1050 Anode for Aluminum Air Battery with KOH Electrolyte

Brahim Idir,[1,*] Mustapha Djama,[1] Djouher Addadj,[1,2] Dalila Boughrara,[3] Lynda Benhaddad,[4] and Amel Kouache[1]

[1]*Research center in industrial technologies (CRTI), P.O. Box 64, Cheraga 16014 Algiers, Algeria*
[2]*Solid State Energy and Electrochemistry Laboratory, Department of Process Engineering, Faculty of Technology, U.F.A. Sétif 1, Sétif,19000, Algeria*
[3]*Physics and Chemistry of Materials Laboratory, Mouloud Mammeri University of Tizi-Ouzou, P.O. Box 17 RP, Tizi-Ouzou 15000, Algeria*
[4]*Laboratory of Materials and Environmental Sciences, Department of Materials Sciences, Faculty of Sciences, University of Algiers 1 Benyoucef Benkhedda, 02 rue Didouche Mourad, 16000 Algiers, Algeria*

*Corresponding Author, Tel.: +213550737152
E-Mail: idirbrahim2016@gmail.com

Received: 22 July 2024 / Received in revised form: 9 November 2024 / Accepted: 11 November 2024 / Published online: 30 November 2024

Abstract- This work addresses the issue of anode corrosion in an aluminum-air battery operating with aqueous alkaline electrolytes. To avoid this problem, an additive known to be an amphoteric surfactant was used. To this end, the surfactant cocamidopropyl betaine (CAPB) was examined as a corrosion inhibitor for the anode of the aluminum-air battery in a 1 M KOH solution. This investigation includes various techniques such as gravimetric measurements, potentiodynamic polarization, electrochemical impedance, surface analysis, and theoretical calculations. The gravimetric tests have shown that the corrosion rate (CR) of aluminum significantly decreases with the addition of CAPB molecules. Polarization curve analysis shows that CAPB acts as a cathodic inhibitor, and EIS data indicate a notable increase in polarization resistance with higher inhibitor concentration. Electrochemical results indicate that the CAPB additive provides substantial anticorrosion protection. At its optimal concentration, CAPB achieves an inhibition efficiency of 84.73%, and even at elevated temperatures (55°C), the efficiency remains around 70%. CAPB adsorption follows the Langmuir isotherm, combining both physisorption and chemisorption, with a primary emphasis

on physical adsorption. To assess the inhibitory effect of the CAPB additive, the surface features and depth profiles are analysed. The formation of a surfactant-based layer is confirmed through FTIR-ATR. Based on the review of the various experimental and theoretical results, a mechanism of inhibition of the surfactant CAPB is proposed.

Keywords- Aluminium-air battery; Surfactant; Cocamidopropyl betaine; Corrosion Inhibition; DFT

1. INTRODUCTION

The development of clean energy technologies has become very significant due to the global need to reduce strong dependence on traditional fossil energy sources and as a means of alleviating environmental pollution. Concerning emerging technologies, metal-air batteries based on Mg, Zn, and Al have attracted significant attention from the scientific community [1,2]. The aluminum-air (Al-air) battery is a type of metal-air battery that emerges as a possible fuel cell. It uses atmospheric oxygen as the cathode material and aluminum as the anode reactant. The superiority of the Al-air batteries varies from their lightweight design to high specific energy and enhanced safety features [3]. The use of alkaline electrolytes in Al-air batteries is essential for achieving high energy density. However, a major drawback of employing alkaline electrolytes in these systems is the occurrence of undesired hydrogen evolution reactions at the anode, which significantly lowers the overall specific capacity of the battery [3]. Therefore, at present, the issue of ensuring the inhibition of the hydrogen generation reaction at the aluminum anode and enhancing the specific capacity of the battery has become quite acute. Numerous alloying elements have been suggested to address the corrosion issue associated with pure aluminum. Potential candidates include gallium, indium, magnesium, thallium, tin, manganese, zinc and lead have shown relative effectiveness [4]. The hydrogen over potential of these alloying elements is higher, which reduces the hydrogen release and self-corrosion process. It should be noted, however, that this approach, in most cases, leads to a price hike for the material.

Several recent studies have shown that the inclusion of additives in the electrolyte provides a valuable means to prevent undesired hydrogen evolution reactions at the anode, but without lowering the activity. Inorganic compounds have received increased attention from researchers for effectively protecting aluminum alloys in alkaline media. Some examples of inorganic protective compounds are zinc oxide [5], sodium silicate [6], and sodium stannate [7]. Other than that, the study also considers organic corrosion inhibitors like polyvinyl alcohol (PVA) [8], plant extracts [9], methanol [10], agar [11], and surfactants as barrier-type inhibitors [12]. Surfactant molecules are amphiphilic; therefore, they are very strongly predisposed to adsorption at interfaces. As a result, when surfactants adsorb onto the aluminum surface, they form a physical barrier that markedly decreases the level of corrosion. A variety of cationic, anionic, and non-ionic surfactants have been employed as corrosion inhibitors for aluminum. [13,14]. Studies suggest that surfactants can lower aluminum's self-corrosion rate in acidic or

alkaline environments by covering active surface sites [13,14]. However, most research has focused on experimental corrosion inhibition of aluminum alloys, and the influence of surfactant molecular structure on inhibition remains unclear. Clarifying this relationship could be crucial for selecting effective inhibitors for aluminum-air batteries. The novelty of this work lies in combining experimental findings such as mass loss, electrochemical, and surface analyses with a computational approach using DFT to provide a deeper understanding of the corrosion inhibition mechanism of the CAPB compound.

Notably, as far as we know, there has been no published research on the use of the amphoteric surfactant Cocamidopropyl Betaine (CAPB) as a corrosion inhibitor for aluminum in an alkaline environment. CAPB is an organic compound obtained from the combination of coconut oil and dimethyl amino propyl amine [15]. The unique reason for broad application in the cosmetic industry is that CAPB has a better conditioning property and is milder than others. It is categorized as a zwitterionic surfactant, containing both a carboxylate anion and a quaternary ammonium cation [16,17]. Amphoteric surfactants can be further classified into two categories: amino acid-based [18] and betaine-based [19,20]. Betaine-based surfactants are soluble in acidic, alkaline, and neutral environments, whereas amino acid-based surfactants typically reach saturation near their isoelectric point.

Biodegradation and toxicity are two essential aspects to be discussed to ensure safety in industrial applications. Aerobic biodegradation testing showed a high rate of biodegradation of CAPB, i.e., 100% in 28 days, showing that it is pretty easily biodegraded with rapid mineralization and meets the necessary 60% biodegradation within less than seven days. Moreover, CAPB quickly degrades anaerobically. Toxicity studies have found that CAPB is nontoxic, with acute LD50 ranging from 2000 to 8000 mg/kg in rats [20].

This research aims to explore the corrosion inhibition of AA1050 aluminum alloy in a corrosive solution 1 M KOH by using Cocamidopropyl Betaine (CAPB). This study will be done through detailed analysis by gravimetric measurements, electrochemical techniques, surface characterization, and theoretical modeling approaches. The electrochemical techniques employed include Open Circuit Potential (OCP), Electrochemical Impedance Spectroscopy (EIS), and Potentiodynamic Polarization (PDP) measurements. The AA1050 aluminum alloy surface was characterized using optical micrographs, profilometry measurements, and attenuated total reflection (ATR) techniques with and without the surfactant in the corrosive solution. The adsorption of CAPB molecules on the aluminum alloy was further examined through Density Functional Theory (DFT) calculations.

2. EXPERIMENTAL SECTION

2.1. Materials and solutions

The aluminum samples used for corrosion studies are of AA 1050 grade, sourced from PIM Algeria, and belong to the 1000 series. The composition of the commercial aluminum

alloy is as follows: Zn 0.05%, Mn 0.05%, Si 0.25%, Fe 0.4%, Cu 0.05%, Mg 0.05%, Ti 0.05%, with the remainder being aluminum. A working electrode was prepared in the form of a circular rod with a surface area of 1 cm². Before each experiment, the exposed surface of the working electrode was mechanically polished using emery papers, followed by rinsing with distilled water. The corrosive medium and the blank solution consisted of a basic solution of 1 mol L^{-1} KOH, prepared by diluting 99% potassium hydroxide with distilled water. The solutions were aerated naturally and stirred magnetically to ensure homogeneity. The Cocamidopropyl Betaine (CAPB) used in this study is commercially available.

2.2. Gravimetric measurements

The dimensions of the aluminum coupon used in the gravimetric study were 2.5 cm in length, 2.5 cm in width, and 0.046 cm in thickness. To prepare the coupons, emery papers with different grades were utilized for abrasion. After the abrasion process, the coupons were degreased with acetone and dried at room temperature. The gravimetric tests were conducted at room temperature, with an immersion duration of 2 hours. The corrosion rate (CR) and inhibition efficiency (g%) were calculated using the following equations:

$$IE\% = (1 - \frac{W_1}{W_2}) \times 100 \quad (1)$$

$$\theta = 1 - \frac{W_1}{W_2} \quad (2)$$

$$CR\ (mg\ cm^{-2}\ h^{-1}) = \frac{W}{A\ t} \quad (3)$$

where, W_1 and W_2, represent the weight losses (in milligrams) for aluminum in the presence of the inhibitor and its absence in a KOH solution, respectively;

θ, is the degree of surface coverage of the inhibitor;

A, represents the area of the aluminum coupon in cm^2;

t represents the duration of immersion in hours;

W represents the weight loss of aluminum after time *t*.

2.3. Electrochemical methods

Electrochemical assessments were performed using an Autolab instrument. All recorded data were analysed and processed using the NOVA 2.0 software. These measurements were conducted using a traditional three-electrode arrangement, where the aluminum sample acted as the working electrode, a saturated $Hg/Hg_2Cl_2\ /Cl^-$ electrode (SCE; E_{SCE} = 0.244 V) served as the reference electrode, and a graphite electrode functioned as the counter-electrode.

The open circuit potential (OCP) of AA 1050 aluminum was monitored for a duration of 3600 seconds before proceeding with additional electrochemical characterization of the system. To examine the effect of the surfactant, the analysis included both KOH alone and KOH solutions containing different concentrations of the surfactant.

Potentiodynamic polarization curves were recorded by varying the potential from - 300 to + 500 mV versus OCP, and the scanning rate was set to 1 mV s^{-1}.

The inhibition efficiency from polarisation curves data (η_P) is calculated using the following equation [21]:

$$\eta_P = \frac{i_{corr(0)} - i_{corr\,(Inh)}}{i_{corr(0)}} \times 100 \quad (4)$$

where, $i_{corr(0)}$ and $i_{corr\,(Inh)}$ are corrosion current densities of uninhibited and inhibited solutions, respectively.

The impedance spectra were obtained after immersing the specimens for a duration of 3600 seconds. During this time, the OCP values reached a stable state. The measurements were conducted over a frequency range of 100 kHz to 10 mHz, with 6 points per decade. An AC excitation signal with a 10 mV amplitude was applied. The inhibition efficiency (η_R) from the EIS method was calculated using the formula shown below [22]:

$$\eta_R = \frac{R_{p(inh)} - R_{p(0)}}{R_{p(inh)}} \times 100 \quad (5)$$

Here, $R_{p(inh)}$ and $R_{p(0)}$ represent the polarization resistances of the AA 1050 aluminium alloy in 1.0 M KOH, with and without inhibitor, respectively.

2.4. Surface analysis

The surfaces of the aluminum samples were analysed and discussed after being immersed for 12 hours in a 1.0 M KOH solution, both with and without CAPB at its optimal concentration of 0.009 M. The samples were initially polished with various grades of emery paper to obtain a mirror-like finish. They were then rinsed with bi-distilled water, degreased with acetone, and immersed in the test and inhibited solutions at room temperature. After 12 hours of immersion, the specimens were taken out, cleaned, dried, and analyzed using optical microscopy (OM) to observe the surface morphologies.

The surface roughness of the corroded and inhibited aluminum samples after immersion was also analyzed using profilometry. Additionally, Attenuated Total Reflectance (ATR) spectroscopy was employed to identify the functional groups of CAPB and those of the layer adsorbed on the AA1050 surface, utilizing the Cary 630 instrument from Agilent Technologies.

2.5. Computational modeling

Quantum chemical calculations were conducted using Density Functional Theory (DFT) within the Spartan 08 software package, applying the B3LYP/6-31G(d, p) level of theory. Structural optimizations were performed in an aqueous phase, as this theoretical approach effectively provides accurate electronic properties for various organic molecules [23]. Key parameters, including the energy of the highest occupied molecular orbital (E_{HOMO}), the energy of the lowest unoccupied molecular orbital (E_{LUMO}), and dipole moments (μ), were determined.

Furthermore, absolute electronegativity (χ), hardness (η), global electrophilicity (ω), and global nucleophilicity (ε) were computed using the respective equations.

$$\chi = \frac{I+A}{2} \quad (6)$$

$$\eta = \frac{I-A}{2} \quad (7)$$

Where the ionization potential $I = -E_{HOMO}$ and electron affinity $A = -E_{LUMO}$.

The global electrophilicity index (ω) is defined as follows [24]:

$$\omega = \frac{\chi^2}{2\eta} \quad (8)$$

The inverse of electrophilicity (1/ω) is referred to as nucleophilicity (ε). To better understand the ability of inhibitor molecules to interact with aluminum atoms and to predict the most favorable adsorbed inhibitor, Pearson [24] showed that the fraction of electrons transferred (ΔN) between the inhibitor molecules and the metal atom can be computed using the following equation:

$$\Delta N = \frac{\chi_{Al}-\chi_{inh}}{2(\eta_{Al}+\eta_{inh})} \quad (9)$$

In this equation, χ_{Al}, χ_{inh}, η_{Al}, and η_{inh} denote the electronegativities and hardness values of aluminium and the inhibitor molecules, respectively.

3. RESULTS AND DISCUSSION

3.1. Weight loss method

Table 1 presents the determined values of corrosion rates (CR), inhibition efficiency (%IE), and the degree of surface coverage (θ) for the aluminum/KOH solution systems, both in the presence and absence of the CAPB inhibitor at 298 K.

Table 1. Parameters obtained from gravimetric tests for AA1050 in 1 M KOH solution with varying concentrations of CAPB at 298 K are as follows:

C_{KOH} (mol L^{-1})	C_{inh} (mol L^{-1})	C_R (mg cm^{-2} h^{-1})	η_G (%)	θ
1	0	2.28	/	/
	0.001	1.045	54.12	0.541
	0.003	0.885	61.24	0.612
	0.006	0.668	70.65	0.707
	0.009	0.417	81.73	0.817

Table 1 clearly shows that as the concentration of CAPB increases, the corrosion rate decreases. Consequently, the percentage of inhibition efficiency rises with the addition of the inhibitor. These findings highlight the effectiveness of CAPB in mitigating aluminum

corrosion across all alkaline solutions tested. This indicates that the CAPB inhibitor in the KOH solution effectively prevents aluminum corrosion, with its protective efficacy being directly related to the concentration of CAPB used. Notably, at the optimal CAPB concentration of 0.009 M, the corrosion inhibition efficiency reached 81.73%.

3.2. Electrochemistry measurements

3.2.1. Open circuit potential

Figure 1(a) illustrates the time-dependent behavior of the open circuit potential (OCP) for the AA 1050 aluminum alloy immersed in a 1.0 M KOH solution, comparing conditions both with and without various concentrations of the CAPB surfactant. The measurements were conducted at 298 K. Within the initial 1000 seconds of immersion in the KOH solution, the corrosion potential (E_{corr}) of aluminum decreases significantly. This decrease in potential indicates that the electrode is being activated, which typically occurs because the initial oxide film covering the aluminum surface begins to dissolve. This dissolution exposes active sites on the aluminum, making it more susceptible to corrosion. However, after approximately 3000 seconds, the corrosion potential reaches a stable equilibrium at around -1.6V (SCE). The stabilized potential at this value indicates the formation of a protective passive layer on the aluminum surface. This layer serves as a barrier, preventing direct interaction between the metal and the corrosive environment, thereby efficiently reducing corrosion [25-27].

With the addition of the surfactant to the corrosive solution, the potential initially rises over the first 250 seconds before stabilizing. This initial increase indicates a transient response, reflecting the interaction between the surfactant molecules and the metal surface. It suggests that the surfactant molecules are forming a protective layer, which contributes to inhibiting the corrosion process. The minor decrease in the open circuit potential (OCP) compared to the uninhibited solution implies that the surfactant influences the system's electrochemical behavior. This potential shift can be linked to the preferential adsorption of surfactant molecules onto the metal surface, which alters the corrosion kinetics. Additionally, as the concentration of CAPB increases, the potential tends to move toward more negative values. This behavior indicates that higher concentrations of the surfactant enhance the inhibition effect on the corrosion process. The denser and more stable protective layer formed by surfactant molecules on the metal surface reduces the corrosion rate, causing the potential to shift towards more cathodic values.

The open circuit potential (OCP) reaches an equilibrium state after 3000 seconds of immersion, regardless of the concentration of CAPB. This observation suggests that the electrochemical behaviour of the system has become stable, indicating that the corrosion process has reached a steady state. At this point, the OCP remains relatively constant. However, the most negative potential value of -1.72 V (ECS) is observed when the concentration of CAPB is 0.009M. This suggests that the surfactant achieves maximum effectiveness in

reducing the corrosion potential at this particular concentration. At this level, it is likely that the surfactant molecules create a more efficient and robust protective layer on the metal surface, resulting in stronger inhibition of the corrosion process.

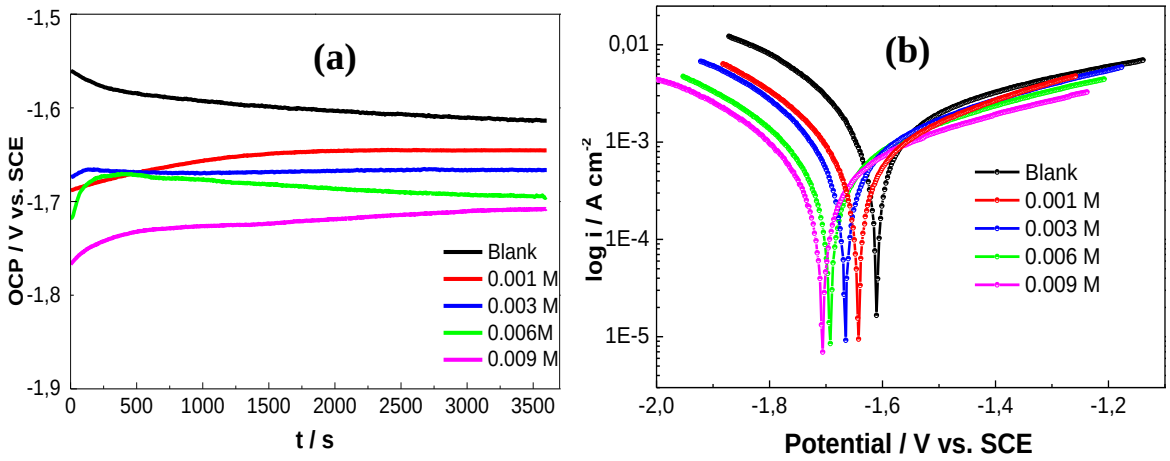

Figure 1. (a) Open circuit potential (OCP) scanning and (b) Potentiodynamic polarization curves for AA1050 aluminum corrosion in 1 M KOH solution with and without various concentrations of CAPB surfactant at 298 K

3.2.2. Potentiodynamic polarization

Polarization measurements were carried out in a 1.0 M KOH solution to evaluate the effect of varying concentrations of the surfactant on the corrosion behavior of AA 1050 aluminum alloy. These measurements were taken both with and without the surfactant, as illustrated in Figure 1(b). The data from the anodic and cathodic branches were analyzed using data fitting techniques, and several parameters were obtained. These include the corrosion current density (i_{corr}), corrosion potential (E_{corr}), cathodic (β_c) and anodic (β_a) Tafel slopes, and the inhibition efficiency percentage (η_P), as summarized in Table 2.

The anodic and cathodic Tafel slopes provide valuable insights into the electrochemical reactions occurring on the surface of AA 1050 aluminum alloy. The anodic currents primarily stem from the oxidation of aluminum, leading to the release of Al^{3+} ions, while the electrons generated in this oxidation are used in the reduction of dissolved hydrogen at the cathodic site, producing cathodic currents. As shown in Figure 1(b), increasing surfactant concentration shifts both anodic and cathodic curves to lower current densities relative to the blank solution, suggesting that the surfactant significantly hinders aluminum dissolution and slows the hydrogen reduction reaction. Increasing the concentration of the inhibitor further amplifies its corrosion protection, as indicated by a drop in corrosion current. This reduction is due to the inhibitor molecules adsorbing onto active sites on the aluminum alloy surface [28]. The surfactant's unique dual-structure, with a hydrophilic polar head and a hydrophobic non-polar tail, explains its adsorption behavior on the alloy's surface. The hydrophilic portion anchors

the molecule to the metal surface, while the hydrophobic section forms a protective, water-resistant layer. This layer effectively shields the metal from the corrosive environment, thereby reducing corrosion significantly [29].

Table 2. Tafel parameters of AA1050 aluminum alloy in 1 M KOH solution in the absence and in the presence of different concentrations of CAPB surfactant recorded at 298 K

Surfactant concentration (mol L^{-1})	**E_{corr} (V/ECS)**	**i_{corr} (mA /cm^2)**	**β_a (V/dec^{-1})**	**$-\beta_c$ (V/dec^{-1})**	**η_P (%)**
0	-1.612	3.46	0.328	0.442	/
0.001	-1.642	1.45	0.318	0.423	58.09
0.003	-1.664	1.21	0.287	0.328	65.03
0.006	-1.692	0.88	0.256	0.244	74.56
0.009	-1.705	0.53	0.235	0.228	84.68

The results suggest that Cocamidopropyl Betaine (CAPB) primarily acts as a mixed-type inhibitor in KOH solution, as the E_{corr} displacement remains below 85 mV [30]. This behavior aligns with our previous findings on carbon steel in NaCl, where CAPB similarly demonstrated mixed inhibition characteristics [23]. The observed shift of Ecorr to more negative values with increasing CAPB concentration indicates an enhanced cathodic effect, though without a clear dominance of either cathodic or anodic influence, supporting its classification as a mixed-type inhibitor.

Moreover, the decline in both cathodic and anodic Tafel slopes, shown in Table 2, indicates that CAPB effectively slows the reaction rates for both anodic and cathodic processes, thus reducing the overall corrosion rate. At a concentration of 0.009 mol L^{-1}, the inhibitor achieves an impressive efficiency of 84%, bringing i_{corr} down to 0.53 mA cm^{-2}, which highlights CAPB's effectiveness in mitigating aluminum corrosion in alkaline KOH. This improvement in efficiency, along with the reduction in i_{corr}, suggests that CAPB may form a protective layer on the aluminum surface, thereby enhancing its corrosion resistance in the KOH environment.

3.3. EIS measurements

To assess the corrosion inhibition effectiveness of the CAPB surfactant on aluminum alloy corrosion in both uninhibited and inhibited solutions, electrochemical impedance spectroscopy (EIS) measurements were performed. Figure 2(a) illustrates the Nyquist plots for an aluminum alloy immersed in a 1.0 M KOH solution, both without and with various concentrations of the CAPB surfactant. All plots show a similar elliptical shape. This observation is consistent with previous studies on aluminum in alkaline solutions [31,32].

The impedance spectrum of the aluminum alloy displays three characteristic features: (i) a pronounced capacitive loop at high frequencies, (ii) a smaller inductive loop at intermediate frequencies, and (iii) an additional capacitive loop at low frequencies. The parameters derived

from electrochemical impedance spectroscopy (EIS) were interpreted using an appropriate equivalent electrical circuit (EEC), as shown in Figure 2(b), with the corresponding values detailed in Table 2.

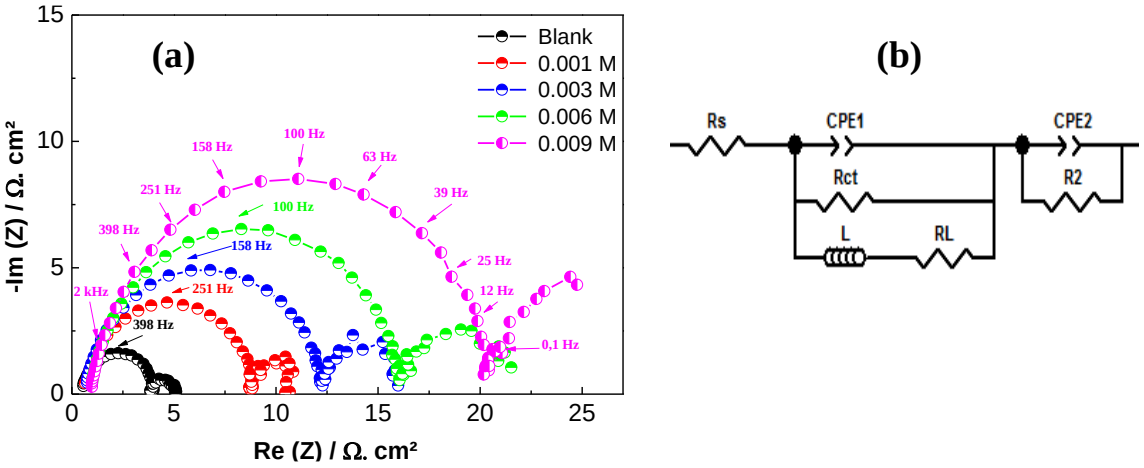

Figure 2. (a) Nyquist diagrams and (b) Electrical Equivalent Circuit (ECC) of AA1050 aluminum in 1 M KOH solution with and without CAPB surfactant

The equivalent electrical circuit (EEC) consists of three components: R_e, CPE_1, and R_{ct}. R_e represents the electrolyte resistance, CPE_1 signifies the deviation from ideal behavior of the double-layer capacitance (C_{dl}) and takes into account surface heterogeneities, and R_{ct} represents the charge transfer resistance. The significant capacitive loop observed at high frequencies, represented by CPE1 in parallel with R_{ct}, is attributed to the redox reaction between Al and Al^+. This charge transfer process is regarded as the rate-limiting step [33].

The resistance value obtained from the intersection of the capacitive loop with the real axis reflects the charge transfer resistance of the Al/Al^+ system. Additionally, at medium frequencies, the observed inductive loop, depicted by an inductance L in series with its resistance R_L can be associated with the adsorbed intermediates that occur during the dissolution process on the aluminum alloy's surface. These intermediates contribute to the impedance response and influence the overall corrosion behaviour [10]. The low-frequency capacitive loop, represented by CPE_2 in parallel with R_2, can be associated to the $Al^+ \leftrightarrow Al^{3+}$ reaction. As reported in the literature, this suggests the involvement of a redox reaction between aluminum (Al) and aluminum ions (Al^{3+}) [34].

Figure 2(a) reveals that the diameter of the initial capacitive loop expands with increasing surfactant concentration, indicating improved corrosion resistance of aluminum in the KOH medium. This observation is supported by data in Table 3, which shows that adding the surfactant leads to higher charge transfer resistance values. The larger capacitive loop suggests that a more protective layer forms on the aluminum surface, likely due to surfactant adsorption, which effectively reduces aluminum's self-corrosion. Additionally, the disappearance of the

inductive loop at higher surfactant concentrations indicates that the inhibitor minimizes the buildup of intermediate corrosion products on the aluminum surface [33]. The measured electrolyte resistance (R_e) is higher in solutions containing the surfactant CAPB than in the KOH-only solution. This increase in R_e is likely due to a reduction in electrolyte conductivity introduced by the surfactant [35].

Table 3. EIS data for the AA1050 aluminum alloy in a 1 M KOH solution at various concentrations of CAPB at 298 K

C (mol L^{-1})	**0**	**0.001**	**0.003**	**0.006**	**0.009**
R_e **(Ω cm^2)**	0.49	0.69	0.64	0.87	0.91
R_{ct} **(Ω cm^2)**	3.57	8.20	11.92	15.46	19.43
CPE_1 **(μΩ^{-1} S^{n}cm^{-2})**	88.31	88.6	118.3	124.37	154.25
n_1	0.94	0.92	0.88	0.88	0.88
L **(H cm^2)**	0.13	1.74	2.79	5.13	8.78
R_L **(Ω cm^2)**	16.99	38.03	59.33	75.35	95.2
CPE_2 **(μΩ^{-1} S^{n}cm^{-2})**	1.282	0.81	0.86	0.82	0.85
n_2	0.66	0.73	0.78	0.75	0.59
R_3 **(Ω cm^2)**	1.8	4.19	8.33	10.65	16.52
R_P **(Ω cm^2)**	4.75	10.93	18.25	23.47	32.63
η_R **(%)**	/	56.54	73.97	79.76	85.44

The Chi-square (χ^2) values of around 10^{-3} confirm the validity of the selected equivalent circuit model. The polarization resistance (R_P) is expressed as:

$$R_P = \frac{R_{tc} \times R_L}{R_{tc} + R_L} + R_2 \quad (10)$$

Table 3 shows an inverse relationship between corrosion current density and polarization resistance. As surfactant concentration increases, polarization resistance (R_P) improves, likely due to CAPB adsorption, which hinders corrosive species at the aluminum surface and promotes the detachment of water molecules from the metal interface, enhancing corrosion resistance [35-37].

3.4. Adsorption isotherm

In corrosion inhibition studies, it is well understood that the inhibition mechanism involves the adsorption of inhibitor molecules onto the metal surface. To gain a comprehensive understanding of this process, it is essential to use appropriate adsorption isotherms. These isotherms provide valuable insights into the effectiveness of corrosion inhibitors by revealing how the inhibitor molecules interact with the metal surface. The analysis typically involves fitting experimental surface coverage data to different isotherm models and selecting the one with the highest regression coefficient to describe the adsorption behavior accurately. In some cases, multiple isotherm models may be applied without explicitly identifying the best fit,

especially when the focus is on examining specific parameters associated with a particular model. In this research, the experimental data were evaluated using several adsorption isotherm models, including Langmuir, Temkin, Freundlich, Flory-Huggins, and Al-Awady.

3.4.1. Langmuir

The Langmuir model, given by Equation (11), describes the correlation linking inhibitor concentration (C) to surface coverage (θ) on the metal surface:

$$C\left(\frac{1-\theta}{\theta}\right) = K^*(T) \tag{11}$$

In this equation, *K* (T)* represents a temperature-dependent constant that is inversely related to the equilibrium constant of the adsorption-desorption process ($K_{ads}=1/K^*$). The linearized form of the Langmuir equation, Eq. (12), can be used to generate a linear plot of C/θ against C, as illustrated in Figure 3.

$$\frac{C}{\theta} = \frac{1}{K_{ads}} + C \tag{12}$$

Here, C refers to the inhibitor concentration, θ indicates the surface coverage, and K_{ads} represents the adsorption equilibrium constant, which signifies the strength of adsorption between the inhibitor molecules and the metal surface.

The surface coverage (θ) refers to the fraction of the metal surface that is occupied by inhibitor molecules and can be determined using Eq. (13):

$$\theta = \frac{IE(\%)}{100} \tag{13}$$

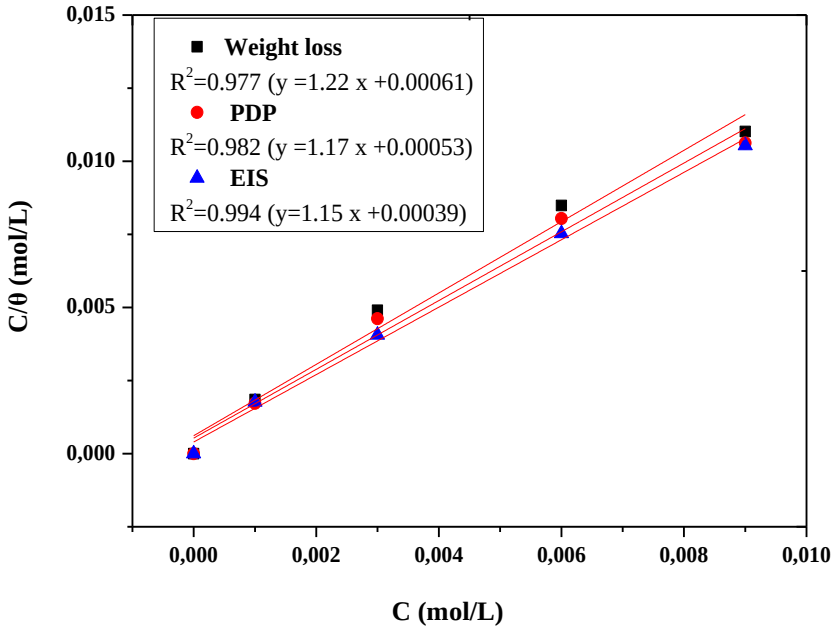

Figure 3. Langmuir adsorption isotherms of CAPB on AA1050 aluminum alloy surface in 1 M KOH solution

The plots of C/θ vs. C, generated using θ values determined from the different methods, are presented in Figure 3.

The R^2 value obtained, which is close to 1, indicates a solid correlation between the experimental data and the Langmuir adsorption model, suggesting that the adsorption of the surfactant CAPB onto the surface of the AA 1050 aluminum alloy adheres to this model. It is important to note that the slope of the linear regression line shows a slight deviation from unity, indicating a minor departure from the ideal Langmuir behavior. Literature reports support these findings, providing evidence of significant interactions between the surfactant molecules and the aluminum alloy surface, resulting in the formation of an inhibiting film that corresponds to a monolayer [39]. Moreover, it is observed that there is no interaction among the adsorbed surfactant molecules on the metal surface [19]. However, numerous studies have shown that larger molecules, such as polymers and polar organic compounds, can exhibit either attractive or repulsive interactions with one another [40,41].

The value of K_{ads} can be determined from the intercept of the linear portion of the C/θ vs. C curve, and the corresponding standard free energy of adsorption (ΔG^0_{ads}) can be calculated using the following equation [42]:

$$\Delta G^0_{ads} = -RT\,ln\,(55.5 \times K_{ads}) \quad (14)$$

where R is the gas constant, T is the absolute temperature in Kelvin, and 55.5 mol L^{-1} represents the value of water concentration in the solution. In this study, the calculated values of K_{ads} were found to be 2000, 2207.5, and 2948.7 L mol^{-1}, and the ΔG^0_{ads} were found equal to -28.80, -29.05, and -29.76 kJ mol^{-1}, for weight loss, PDP, and EIS respectively. The high value of K_{ads} indicates a strong adsorption capacity of the surfactant molecules on the aluminum alloy surface, while the negative values of ΔG^0_{ads} suggest that the adsorption process is spontaneous.

The literature indicates that, ΔG^0_{ads} values around -20 kJ mol^{-1} or less negative suggest electrostatic attraction between charged inhibitor molecules and the charged metal surface, which points to physical adsorption. Conversely, values nearing -40 kJ mol^{-1} or more negative signify the transfer of inhibitor molecules to the metal surface, resulting in the formation of covalent bonds and indicating chemical adsorption. Values within this range typically suggest a mixed mechanism that encompasses both physicochemical interactions.

In our study, the obtained ΔG^0_{ads} values indicate that CAPB adsorption involves both physical and chemical processes. However, relying solely on adsorption energy cannot specify the adsorption mechanism. Other experiments, such as studying the effect of temperature, are important for understanding the adsorption process. Surfactants typically contain functional groups that can form covalent bonds with metal surfaces, including aluminum alloys. These covalent bonds occur when electrons are shared between the atoms of the surfactant and those of the metal surface, resulting in stronger chemical adhesion. In addition to covalent bonds, surfactants can also interact with aluminum alloy through electrostatic attraction. These interactions rely on the electric charges on the metal surface and the opposing charges of the

surfactant's functional groups. Electrostatic attractions can be particularly significant when the surfactants are charged.

3.5. Influence of temperature and thermodynamic characteristics

The effect of temperature on the inhibition efficiency and corrosion current density values was examined using potentiodynamic curves across a temperature range of 298 to 328 K, both in the absence and presence of 0.009 M CAPB in a 1 M KOH solution. The results are illustrated in Figure 4, while, the data from the anodic and cathodic branches were analyzed through fitting, leading to the determination of several parameters summarized in Table 4.

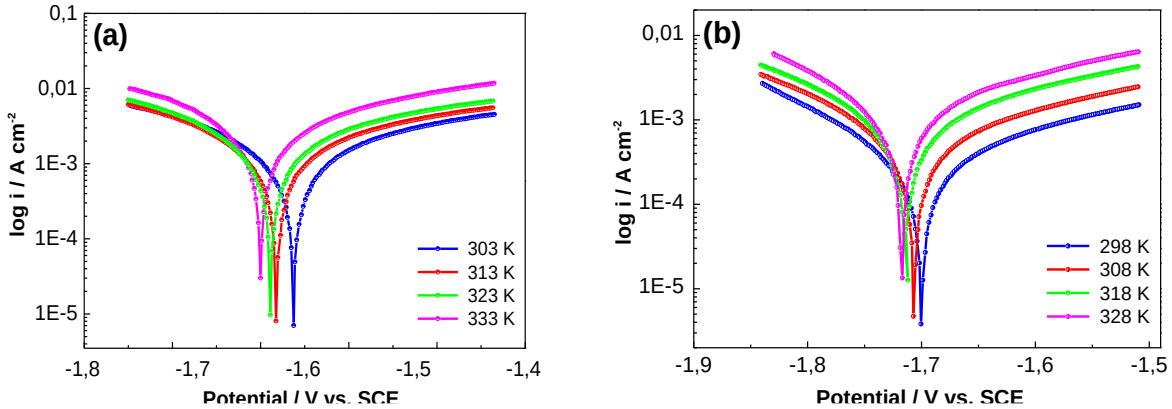

Figure 4. Tafel curves of AA1050 aluminum alloy in (a) 1 M KOH solution and (b) 1 M KOH solution containing 0.009 M of CAPB registered at various temperatures

Table 4. Temperature effect on the corrosion parameters of AA1050 aluminum alloy in 1 M KOH in the absence and presence of 0.009M of CAPB surfactant

T (K)	[CPAB] M	E_{corr} (V/ECS)	i_{corr} (mA /cm^2)	β_a (V/dec^{-1})	$-\beta_c$ (V/dec^{-1})	η_P (%)	θ
298	**0**	-1.612	3.46	0.328	0.442	/	/
	0.009	-1.705	0.53	0.235	0.228	84.7	0.847
308	**0**	-1.625	5.25	0.354	0.449	/	/
	0.009	-1.708	1.09	0.244	0.242	79.23	0.792
318	**0**	-1.631	7.08	0.368	0.452	/	/
	0.009	-1.712	1.9	0.248	0.248	73.11	0.731
328	**0**	1.641	9.85	0.375	0.448	/	/
	0.009	-1.735	3.12	0.256	0.248	68.32	0.683

The rise in temperature led to an acceleration of the corrosion rate in both the inhibited and uninhibited solutions, which consequently reduced the effectiveness of the inhibitor. This is likely because some CAPB molecules desorbed from the active sites, causing a moderate dissolution of the aluminum alloy. It's noteworthy that even at a temperature of 328K, the inhibitor still maintained a significant efficiency of 68.32% at the optimal concentration of CAPB.

The apparent activation energy (E_a) can be determined using the Arrhenius equation:

$$i_{corr} = A \exp(-E_a / RT) \quad (15)$$

In this equation, E_a represents the apparent activation energy, R is the gas constant, and A denotes the Arrhenius pre-exponential factor. By plotting the natural logarithm of the current densities against 1/T, the activation energy can be extracted from the slope, which is given by (−Ea/R).

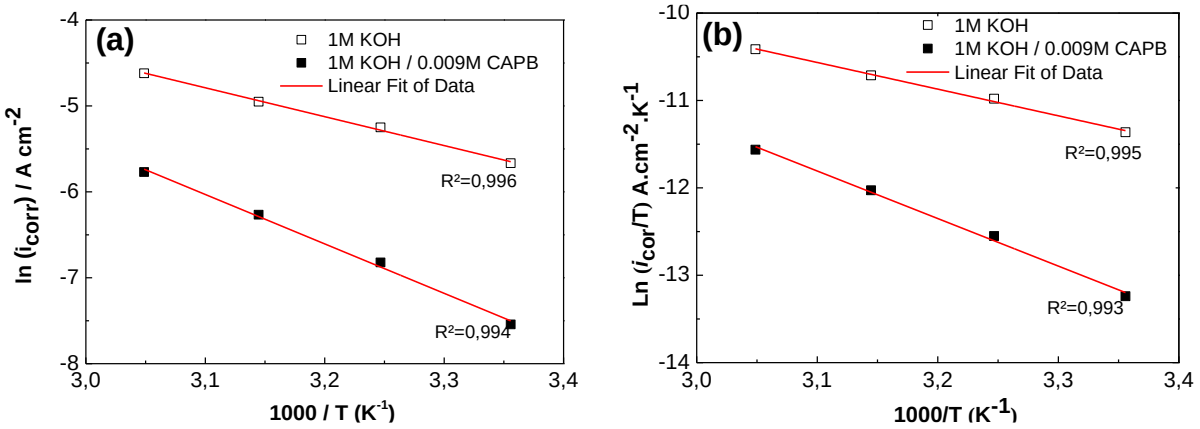

Figure 5. (a) The Arrhenius and (b) the transition state plots for AA1050 aluminum alloy in 1M KOH (blank) and in the solution containing 0.009 M of CAPB surfactant

A straight line was obtained by plotting a graph between ln i_{corr} versus $1/\underline{T}$ as shown in Figure 5(a), with a slope value of E_a/R. As shown the value of E_a for the uninhibited system is 27.98 kJ/mol which is much lower than the value observed for the inhibited system (47.85 kJ/mol). The higher activation energy value for an inhibited system can be explained by the formation of a physical barrier to the transfer of charge and mass, which is created by the adsorbed inhibitor molecules [43]. In fact, using an alternate form of the Arrhenius transition state equation (16), we were able to calculate ΔH_a° and the entropy ΔS_a°:

$$i_{corr} = \frac{RT}{Nh} \exp\left(\frac{\Delta S^\circ_a}{R}\right) \exp\left(-\frac{\Delta H^\circ_a}{RT}\right) \quad (16)$$

where, h is Plank's constant and N is Avogadro's number.

Additionally, a plot of in the ln i_{corr}/T against 1/T gives a straight line with a slope value of ($-\Delta H_a/R$) and an intercept of [In (R/Nh) + ($\Delta S_a/R$)] as shown in Figure 5(b).

The positive values of activated enthalpy, ΔH_a^0 (25.38 and 45.25 kJ/mol for the blank and inhibited solutions, respectively), indicate that the process is endothermic. This means that aluminum dissolution requires more energy to reach the activated state when an inhibitor is present. Additionally, the increase in ΔS_a^0 (becoming more positive) with CAPB (-206.85 and -155.62 J mol^{-1} K^{-1} for the blank and inhibited solutions, respectively) suggests a transition in the dissolution system from a more ordered to a more disordered state. This shift can be attributed to the adsorption of organic inhibitor molecules, which likely replace water molecules on the metal surface through a quasi-substitution process. The adsorption of the inhibitor promotes the desorption of water molecules from the metal surface, thereby increasing the solvent entropy of activation [43].

3.6. Surface analysis

The optical micrographs presented in Figure 6 serve as a valuable tool for examining the surface appearance and corrosion properties of aluminum samples under different conditions. Figure 6(a) illustrates the state of the aluminum surface after immersion in a 1 M KOH solution.

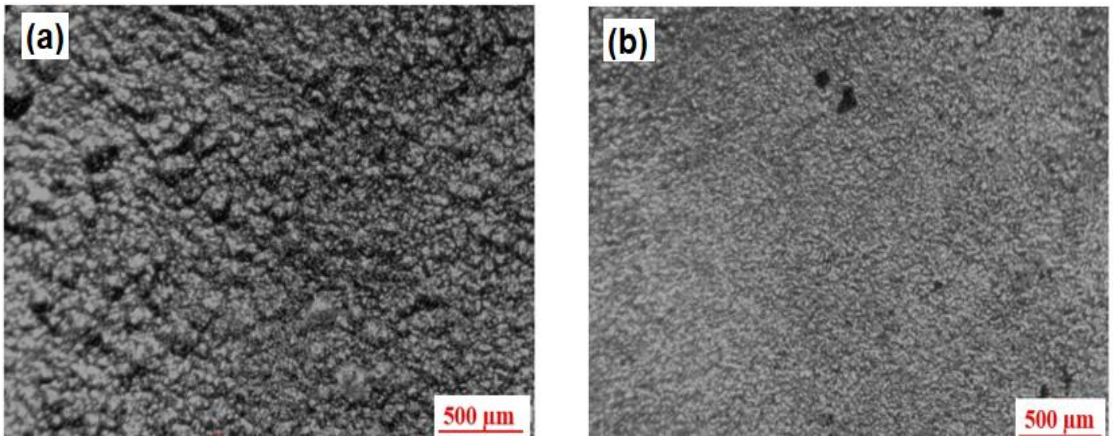

Figure 6. Optical micrographs of the aluminum surface after 12 hours of immersion: (a) in a blank solution, and (b) with 0.009M CAPB surfactant.

The surface has significant damage, with the matrix dissolving quickly, visible coarse deposits, and uneven bumps of different sizes, resulting in a rough texture. On the other hand, Figure 6(b) illustrates the aluminum surface after 12 hours of immersion in a KOH solution containing an optimal surfactant concentration of 0.009 M. The surface appears to be uniformly smooth, with only a few medium-sized deposits. This observation indicates that the surfactant CAPB effectively protected the aluminum surface by forming a protective layer. Figure 7 presents the application of profilometry to assess the impact of inhibitors on the corrosion behaviour of aluminum alloy in various media.

Profilometry is a method used to measure surface properties, such as roughness and topography, which helps us understand the corrosion process.

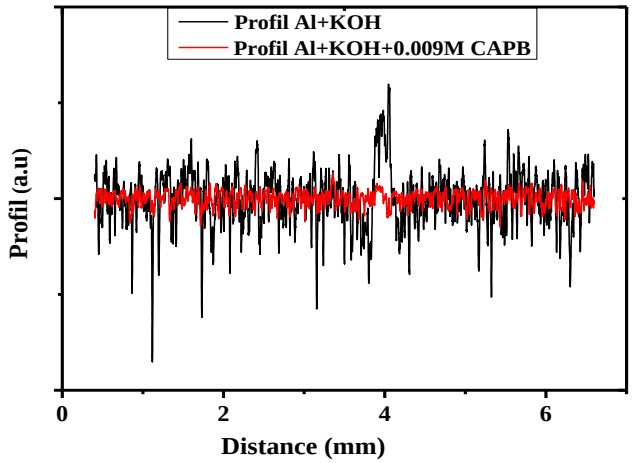

Figure 7. Surface depth profile of AA1050 aluminum alloy samples after 12-hour immersion in 1 M KOH solution and 1 M KOH solution containing the CAPB surfactant.

The profilogram of the corroded sample displays noticeable peaks that represent surface roughness. In contrast, the profilogram of the inhibited sample shows reduced peak height, indicating a decrease in surface roughness due to the protective film created by the surfactant.

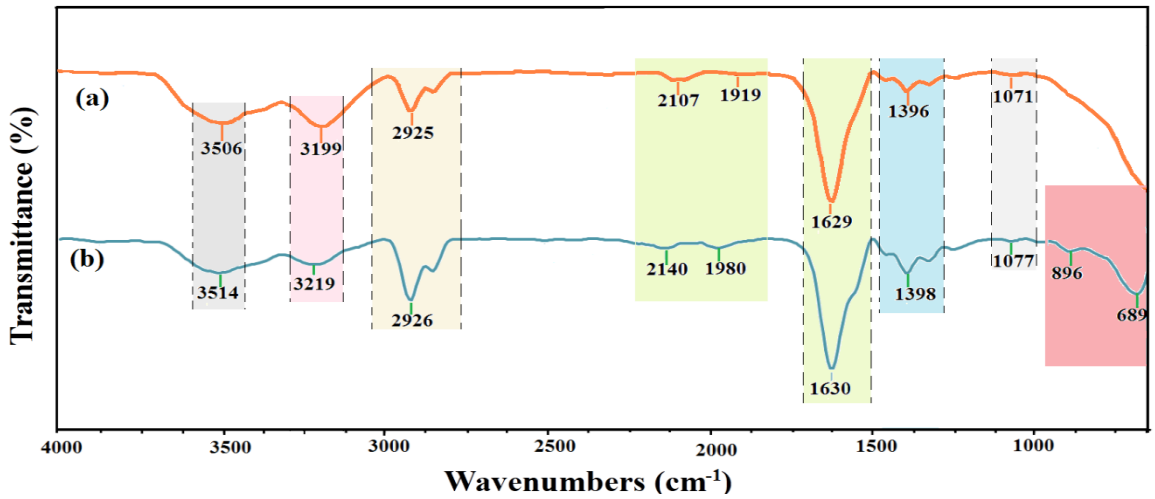

Figure 8. ATR spectrum of (a) CAPB surfactant (b) the film recorded on the aluminium surface after 12-hours of immersion in 1 M KOH containing 0.009M CAPB surfactant

Figure 8 presents the ATR spectra of both the pure surfactant and the adsorbed film on the aluminum surface, with the objective of confirming the effective adsorption of the CAPB surfactant onto the aluminum surface.

Figure 8(a) illustrates the infrared spectrum of the surfactant (CAPB), showing a broad absorption band around 3506 cm^{-1}, corresponding to the OH stretching vibration. The absorption bands at 2925, 2851, and 1464 cm^{-1} are assigned to the C-H stretching vibrations of the -CH_2 group, while the band at 2954 cm^{-1} is linked to the C-H stretching vibration of the methyl group (-CH_3). The amide's C=O and N-H vibrational absorption bands appear at 1629 and 1552 cm^{-1}, respectively [44]. According to the literature, the absorption bands for symmetric carboxylic acids (COO^-) and the C-N stretching vibration of the amide are found within 1340-1300 cm^{-1} and 1418-1375 cm^{-1}, respectively [45]. In this analysis, the COO^- and C-N bonds are recorded at 1331 and 1398 cm^{-1}. Similar bands appear in the spectrum of the layer formed on the aluminum surface, with slight shifts in wavenumbers (Figure 8(b)) and the emergence of two new peaks at lower wavenumbers. These shifts suggest the formation of a surfactant-based film on the aluminum alloy surface, limiting hydrogen release and confirming the effective adsorption of CAPB on the aluminum surface [43].

3.6. Theoretical study and inhibition mechanism

Density Functional Theory has enhanced our comprehension of molecular energy and has demonstrated its utility in examining the reactivity of corrosion inhibitor molecules. This method has emerged as an essential tool for analyzing experimental data and understanding the mechanisms of corrosion inhibition [46].

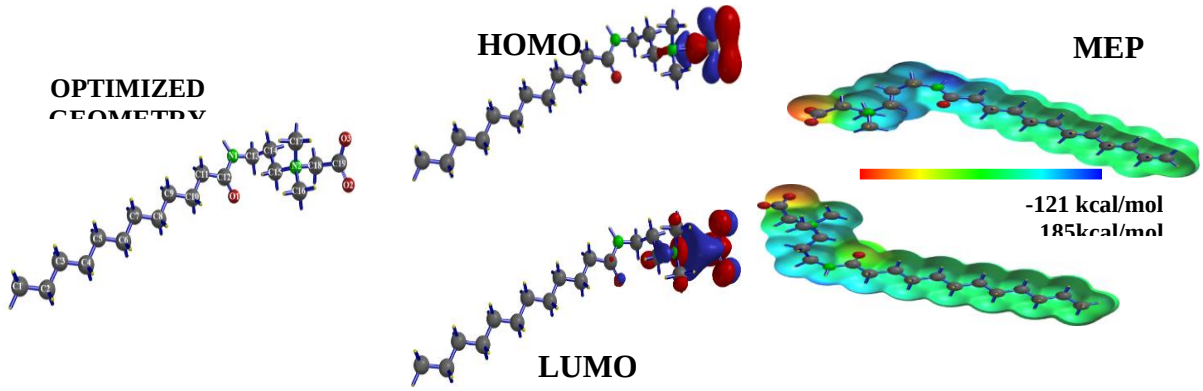

Figure 9. Optimized geometry, frontier orbitals HOMO and LUMO, and MEP surface of the CAPB surfactant

In the following, we aim to examine the molecular and electronic structures of CAPB to elucidate the inhibition mechanism of this compound. Betaines have a nitrogen atom that is fully quaternized and does not have anionic properties in alkaline solutions. This means that betaines exist only as "zwitterions" [20].

Figure 9 illustrates the optimized molecular structure of CAPB, highlighting a polar region that exhibits a preference for polar solvents, particularly water. This polar region is known as

the "hydrophilic part." On the other hand, the nonpolar region is referred to as the "hydrophobic part," which tends to repel polar solvents. Surface coverage primarily occurs through the hydrophilic part, leading to the formation of micelles. This behavior arises because the surfactant reduces its solvation energy by arranging hydrocarbon chains into droplet-like structures. Figure 9 illustrates the electron density distributions of the frontier molecular orbitals in the CAPB molecule. The highest occupied molecular orbital (HOMO) is associated with the molecule's capacity to donate electrons to vacant metal orbitals. Conversely, the lowest unoccupied molecular orbital (LUMO) represents the molecule's ability to accept electrons from occupied metal orbitals. The HOMO orbital is primarily localized on atoms O2, O3, and along the O2-C19-O3 bond, with additional contributions from atom C18, along the C18-N2 bond and the N5-C15 bond. On the other hand, the LUMO orbital is predominantly distributed across atoms O1, C18, C19, N2, C15, O2, and O3. Notably, both the HOMO and LUMO distributions in CAPB are concentrated in the polar hydrophilic fragment.

The results from the DFT calculations indicate a high HOMO energy (-6.25 eV), a small energy difference ΔE (6.87 eV), low hardness η (3.43 eV), and a positive fraction of transferred electrons ΔN (0.21), suggesting a greater global nucleophilic index compared to the electrophilic index. Additionally, CAPB possesses a significantly higher dipole moment of 16.37 Debye, surpassing that of water (μH_2O = 1.84 Debye). This increased dipole moment facilitates the displacement of water molecules from the metal surface. These parameters indicate a robust interaction between CAPB and the aluminum surface, resulting in enhanced inhibition performance.

The electrostatic potential map provides insights into the charge density and electron distribution within the CAPB molecule. This map displays the electrostatic potential values using a color gradient. The red areas indicate regions with the most negative potential, suggesting sites where electrophilic attacks are likely to occur. Conversely, the blue regions represent areas with the highest positive potential, indicating locations favorable for nucleophilic attacks.

According to Figure 9, the oxygen atoms (highlighted in red) have the highest negative electrostatic potential. This indicates that they have an abundance of electrons and are likely to be affected by electrophilic attacks. On the other hand, atoms N5, C8, C9, and C10 have positive electrostatic potentials (highlighted in blue), suggesting that they have a lack of electrons and are susceptible to nucleophilic attacks [47]. The MEP surface presented indicates that the CAPB molecule is more electrophilic because there are more areas of blue color. Additionally, the positive MEP energy is slightly higher than the negative MEP energy. This means that the surfactant molecules exhibit a greater tendency for physical adsorption onto the aluminum surface, aligning with the obtained adsorption isotherm.

Based on both experimental and theoretical findings, we propose a plausible mechanism of inhibition. The surfactant is likely to adsorb to the electrode surface, specifically on the cathode

that activate the reaction of reducing water. The hydrophilic part of the surfactant interacts with the surface of the electrode, while the hydrophobic part extends into the solution, creating a barrier that prevents water molecules from reaching the surface. As a result, the production of hydrogen from aluminum in an alkaline solution is decreased, which improves the efficiency of using AA1050 aluminum as an anode in a 1.0 M KOH solution. However, the smaller OH^- ions can still pass through the protective film. Therefore, the dissolution of aluminum may still occur at a similar rate, resulting in the same level of energy production. This proposed mechanism emphasizes the surfactant's role in creating a safety barrier on the aluminum surface. This protective layer prevents water molecules from accessing the surface and diminishes the occurrence of the hydrogen evolution reaction. The protective film selectively allows OH^- anions to pass through, which enables the controlled dissolution of aluminum. This balance ensures both efficient energy production and inhibition.

4. CONCLUSION

This work investigated the inhibition properties of an amphoteric surfactant called Cocamidopropyl Betaine (CAPB), for corrosion protection of AA1050 aluminum in a 1.0 M KOH alkaline solution. The investigation involved electrochemical measurement, surface morphology analysis, theoretical calculations, and thermodynamic assessment. Based on these analyses, the following conclusions were drawn:

- Gravimetric tests revealed that the corrosion rate (CR) decreased with increasing concentrations of CAPB.
- Analysis of the polarization curves indicated that the surfactant CAPB functions as a cathodic inhibitor. Its inhibition efficiency rises with increasing concentration.
- The EIS plots indicate that the polarization resistance of the AA1050 electrode enhances significantly with higher inhibitor concentrations .
- The adsorption of CAPB adheres to the Langmuir isotherm and involves both physisorption and chemisorption interactions, with a predominant focus on physical adsorption.
- The inhibition efficiency of CAPB is slightly affected by an increase in temperature. At 328K, the inhibition is approximately 70%.
- Surface analysis clearly shows that the presence of CAPB significantly reduces damage to the aluminum surface, which is supported by experimental results.
- Quantum chemical parameters showed a strong correlation with inhibition performance and supported the experimental findings.

Declarations of interest

The authors declare no conflict of interest in this reported work.

REFERENCES

[1] S. Huang, P. Pei, and Z. Wang, J. Electrochem. Soc. 167 (2020) 090538.
[2] M.A. Deyab and M.M. Al-qhatani, ACS Omega 6 (2021) 26640.
[3] Y. Zuo, Y. Yu, H. Shi, J. Wang, C. Zuo, and X. Dong, Membranes 12 (2022) 407.
[4] R. Liang, Y. Su, X.L. Sui, D.M. Gu, G.S. Huang, and Z.B. Wang, J. Solid State Electrochem. 23 (2019) 53.
[5] L. Yang, Y. Wu, S. Chen, Y. Xiao, S. Chen, P. Zheng, J. Wang, and J.E. Qu, Mater. Chem. Phys. 257 (2021) 123787.
[6] O. Lopez-Garrity, and G.S. Frankel, Electrochim. Acta 130 (2014) 9.
[7] C. Lv, Q. Zhang, Y. Zhang, Z. Yang, P. Wu, D. Huang, H. Li, H. Wang, Y. Tang, Electrochim. Acta 417 (2022) 140311.
[8] S. Choi, K. Kim, and J. Kim, J. Mol. Liq. 364 (2022) 120104.
[9] E. Grishina, D. Gelman, S. Belopukhov, D. Starosvetsky, A. Groysman, and Y. Ein-Eli, ChemSusChem 9 (2016) 2103.
[10] J.B. Wang, J. M. Wang, H.B. Shao, J.Q. Zhang, and C.N. Cao, J. Appl. Electrochem. 37 (2007) 753.
[11] W.H. Lee, S.R. Choi, and J.G. Kim, J. Electrochem. Soc. 167 (2020) 110503.
[12] M.A. Deyab, J. Power Sources 412 (2019) 520
[13] N.A.F. Al-Rawashdeh and A.K. Maayta, Anti-Corros. Methods Mater. 52 (2005) 160.
[14] P. Gan, D. Zhang, L. Gao, Z. Xin, and X. Li, Colloids Surf. A Physicochem. Eng. Aspects 670 (2023) 131530.
[15] P. Mehdizadeh, M. Jamdar, M.A. Mahdi, W.K. Abdulsahib, L.S. Jasim, S.R. Yousefi, and M. Salavati-Niasari, Arab. J. Chem. 16 (2023) 104579.
[16] J. F. Fowler, K.M. Zug, J.S. Taylor, F.J. Storrs, E.A. Sherertz, D.A. Sasseville, R.L. Rietschel, M.D. Pratt, C.G.T. Mathias, J.G. Marks, H.I. Maibach, A.F. Fransway, V.A. Deleo, and D.V. Belsito, Dermatitis 15 (2004) 5.
[17] C. Foti, D. Bonamonte, G. Mascolo, A. Corcelli, S. Lobasso, L. Rigano, and G.J. Angelini, Eur. Acad. Dermatol. Venereol. 23 (2009) 204.
[18] B. El Ibrahimi, A. Jmiai, L. Bazzi, and S. El Issami, Arab. J. Chem. 13 (2020) 740.
[19] F. Zhang, X. Li, S. Deng, M. Tang, and G. Du, J. Mater. Res. Technol. 15 (2021) 7050.
[20] M.T. Garcia, E. Campos, A. Marsal, and I. Ribosa, Environ. Int. 34 (2008) 1001.
[21] M.A. Amin, S.S. Abd El Rehim, and H. T. M. Abdel-Fatah, Corros. Sci. 51 (2009) 882.
[22] A.S. Fouda, H.A. Mostafa, F. El-Taib, and G.Y. Elewady, Corros. Sci. 47 (2005) 1988.
[23] M. Djama, L. Benhaddad, B. Idir, N. Achoui, and H. Daifallah, J. Solid State Electrochem. 27 (2023) 2139.
[24] R.G. Pearson, Inorg. Chem. 27 (1988) 1342.
[25] A. Kokalj, Electrochim. Acta 56 (2010) 745.
[26] D.O. Flamini, S. B. Saidman, and J. B. Bessone, Corros. Sci. 48 (2006) 1413.

[27] P. Moises Meza, Int. J. Robotic Eng. 6 (2023) 1.
[28] Z. Moghadam, M. Shabani-Nooshabadi, and M. Behpour, J. Mol. Liq. 242 (2017) 971.
[29] S. Tiwari, C. Mall, and P. Prakash Solanki, Int. J. Eng. Res. Appl. 8 (2018) 61.
[30] E. Ituen, V. Mkpenie, and E. Ekemini, Sci. Afr. 3 (2019) 75.
[31] D.D. Macdonald, Rev. Mechanistic Anal. Electrochem. Impedance Spectrosc. 1990.
[32] A.M. Abdel-Gaber, E. Khamis, H. Abo-ElDahab, and S. Adeel, Mater. Chem. Phys. 109 (2008) 297.
[33] C.M.A. Brett, The Application of Electrochemical Impedance Techniques to Aluminium Corrosion in Acidic Chloride Solution (1990).
[34] C. Verma, P. Singh, I. Bahadur, E.E. Ebenso, and M.A. Quraishi, J. Mol. Liq. 209 (2015) 767.
[35] H.M. Abd El-Lateef, H.S. El-Beltagi, M.E.M. Mohamed, M. Kandeel, E. Bakir, A. Toghan, K. Shalabi, A.H. Tantawy, M.M. Khalaf, Front. Mater. 9 (2022).
[36] A. Singh, K.R. Ansari, M.A. Quraishi, S. Kaya, and P. Banerjee, New J. Chem. 43 (2019) 6303.
[37] A. Mukherjee, and I.N. Basumallick, Complex Behaviour of Aluminium Dissolution in Alkaline Aqueous 2-Propanol Solution (1996).
[38] M. Musah, Y. Azeh, J. Mathew, M. Umar, Z. Abdulhamid, and A. Muhammad, Caliph. J. Sci. Technol. 4 (2022) 20.
[39] A.M. Badiea and K. N. Mohana, Corros. Sci. 51 (2009) 2231.
[40] S.A. Umoren, M.J. Banera, T. Alonso-Garcia, C.A. Gervasi, and M.V. Mirífico, Cellulose. 20 (2013) 2529.
[41] Z. Tao, W. He, S. Wang, S. Zhang, and G. Zhou, Corros. Sci. 60 (2012) 205.
[42] A. Yurt, and Ö. Aykin, Corros. Sci. 53 (2011) 3725.
[43] B. Idir, and F. Kellou-Kerkouche, J. Electrochem. Sci. Technol. 9 (2018) 260.
[44] L. Carolei and I. G. R. Gutz, Talanta 66 (2005) 118.
[45] K.N. Reishus, A. D. Brathwaite, J. D. Mosley, and M.A. Duncan, J. Phys. Chem. A. 118 (2014) 7516.
[46] M.A. Albo Hay Allah, A.A. Balakit, H.I. Salman, A.A. Abdulridha, and Y. Sert, J. Adhes. Sci. Technol. 37 (2023) 525.
[47] W. Daoudi, A. Chaouiki, M. El Mahamdi, K. Zaidi, O. Dagdag, A. Aouinti, Y.G. Ko, M. Abboud, A. Oussaid, and A. El Aatiaoui, J. Adhes. Sci. Technol. 37 (2023) 2944.
[48] Q. Liu, J. Liu, J. Wang, and Y. Chong, J. Mol. Struct. 1274 (2023).